Liquid cell with temperature control for in situ TEM chemical studies

M. Denoual, V Menon, T. Sato, O. de Sagazan, A. W. Coleman, H. Fujita

Liquid cell with temperature control for *in-situ* TEM chemical studies

M Denoual[1,2,3], V. Menon[1], T. Sato[1], O. de Sagazan[4], A. W. Coleman[1,5], H. Fujita[1]
[1]Institute of Industrial Science, The University of Tokyo, 4-6-1 Komaba Meguro-ku, Tokyo, Japan
[2]GREYC-ENSICAEN, Université de Caen Basse Normandie, 6 bd maréchal Juin, 14000 Caen, France
[3]LIMMS, Institute of Industrial Science, 4-6-1 Komaba Meguro-ku, Tokyo, Japan
[4]IETR Groupe microélectronique, Université de Rennes 1, 35000 Rennes, France
[5]Laboratoire Multimatériaux et Interfaces, Université Claude Bernard Lyon 1, 69622 Villeurbanne, France

Email : mdenoual@ensicaen.fr

Abstract:

Liquid cells are hermetically sealed capsules that make it possible to image through liquids at the nanoscale using Transmission Electron Microscopes (TEM). Liquid cells can be passive vessels or integrate electrodes up to now for electrodeposition experiments. Temperature is a key parameter for chemical kinetics of processes. This paper describes a temperature controlled liquid cell for *in-situ* TEM studies. The liquid cell integrates a resistive element for both heating and sensing temperature. A capacitively coupled heat feedback technique is implemented to control the temperature of the liquid cell from room temperature to 100°C with accuracy ±0.1°C. In-situ TEM experiment illustrate the heating capability of such temperature controlled liquid cell while observing at the nanoscale.

Keywords: liquid cell, TEM, temperature control, capacitively coupled heat feedback
PACS numbers:
Submitted to : Measurement Science and Technology

1. Introduction

The physical and chemical properties of matter are intimately related to its structure. Highly driven by nanotechnologies, the study of natural, biological or synthetic material at the nanoscale is a current topic common to a variety of fields including biology, chemistry, medicine and materials science. In their conventional usage, tools such as X-ray diffractometer, Transmission Electron Microscopes (TEM) and Atomic Force Microscopes, enable a static observation of matter at the nanoscale. Among those tools, TEM exhibits the most versatility as an extension of optical microscope at a lower scale and has become standard analytical tool. Yet, the conventional usage does not authorize the study of liquid samples and consequently the access to fundamental process dynamics.

With the development of microfabrication technologies, a dedicated usage for liquid samples, proposed in the 1930's [1, 2], has become possible with a new class of devices referred to as liquid

cells. Those devices enrich TEM with the capability to achieve real-time observation of nanometer-scale dynamic phenomena within fluid media, such observation of liquid samples provides unique insights into life and materials science. Commercial solutions exist based on dedicated perfused holders with silicon microfabricated lids and O-rings assembled at the tip. Those perfused holders usually integrate 3 or 4 electrodes for liquid biasing or heating. The interest in these commercial tools is particularly driven by electrochemical studies [3] in the field of batteries. Alternative solution to the micro-lid type liquid cell associated to a perfused holder is the stand-alone liquid cell type.

Stand-alone liquid cells are capsules or vessels containing the liquid sample and sealed hermetically to prevent evaporation in the high vacuum environment of the TEM. The observation with the electron beam of the TEM is achieved through membranes thin enough to reduce electron scattering and enable high resolution [4, 5]. The thin membranes are usually made out of silicon nitride, even if some development work is being conducted using graphene sheets [6, 7]. The most common process consists in the assembly of two silicon chips with silicon nitride membranes (20 to 200 nm thick) aligned forming the observation hole. The two chips are stacked one over the other with an intermediate spacer material forming the space wherein liquid is sandwiched and the assembly is finally hermetically sealed [4, 5]. The resulting liquid cell allows for the observation of liquid samples even in conventional, non-specialized TEM setups with regular TEM holders. Compared to micro-lid type liquid cell with perfused holder, two-chip liquid cells operate with smaller volumes of liquid and the studied samples can be unloaded from the TEM holder in a non-destructive way.

Observation of liquid samples at the nanoscale has been a breakthrough of the 2000's for the fields of life and material sciences. Nowadays much effort is being expended on recreating the natural or artificial environment of the sample, biological or other, to be able to *in-situ* and *operando* study process dynamics, and to interact with the sample. For this purpose, liquids cells integrating electrodes for electrochemical interaction [8-10] have been proposed.

This work focuses on the achievement of temperature control of the liquid sample in a liquid cell. Some previous work has investigated the temperature effect in similar devices but dedicated to gas study using a micro-machined heater with estimated uncertainty of 10% on temperature [11]. This work proposes a specific design approach dedicated to cells containing liquids associated with a previously proposed heat-feedback technique [12] enabling accurate temperature control at the location of the sample observation. The design can be adapted to various holders as long as they have electrical contacts.

2. Temperature controlled liquid cell

2.1 Design

The device, as with conventional liquid cells, comprises two silicon chips with thin electron transparent silicon nitride membranes forming the observation chamber. The bottom chip with the

resistive element for temperature control and the top chip with the liquid inlet and outlet are assembled and sealed to form an hermetic vessel embedding the liquid medium to be observed; general schematics of the device are illustrated in Figure 1.

The resistive element is integrated inside the liquid chamber in order to control the temperature at the very location of the observation. The center of the observation window is kept without resistive element to remain transparent to the electron beam (e-beam). The central area clear of metal is about 20 µm in diameter. For temperature control, since the resistive element is in direct contact with the liquid medium, the operating voltage has to be kept below the hydrolysis threshold of water, *i.e.* 1.23 V (water-based liquid medium solutions represent the vast majority of the solutions used/of interest).

As a rule of thumb, the higher the thermal insulation is, the less the power required for heating is. The thermal insulation is mainly related to the diameter of the self-sustained membrane and to its thickness. Practical process fabrication considerations enabling high good-die yield fix a membrane radius of 200 µm (r_2). The resistive element for temperature control at the center of the membrane is designed to be 40 µm in radius (r_1). Considering a worst case scenario with the thickest (200 nm) nitride layer, a rough evaluation of the thermal conductance G_{th} using the following formula, $G_{th} = 2\pi \cdot \lambda \cdot t/\ln(r_2/r_1)$ [15], yields to values for a single membrane in the range [7.8-33 µW/K] depending on silicon nitride thermal conductivity ($\lambda_{Si3N4} \in$ [10-43 W/m.K]).

A design margin considering a maximum total thermal conductance of 100 µW/K is applied to encompass process discrepancies, silicon nitride thermal conductivity variations, liquid medium loading and other thermal exchange phenomena. Experimentally for 70 nm and 180 nm thick membrane devices, average thermal conductivities of 7-15 µW/K and 30 µW/K were extracted from measures respectively for liquid cells unfilled with liquid and liquid cells filled with liquid.

The required heating power to ensure temperature variations of up to 100°C can then be derived and yields a maximum Joule power of 10 mW. This required power and the voltage limitation to prevent hydrolysis fix the maximum value for the resistance of the resistive element to about 100 Ω.

Taking into account the resistivity of thin metallic layer deposited, the length and thickness of the resistive element designed to achieve resistance values below 100 Ω, in practice 100 nm thick 6 µm wide metal tracks. A 4-wire resistive element is designed to suppress the effect of contact resistance and conductive paths. The measured resistance then corresponds only to the central circular resistance.

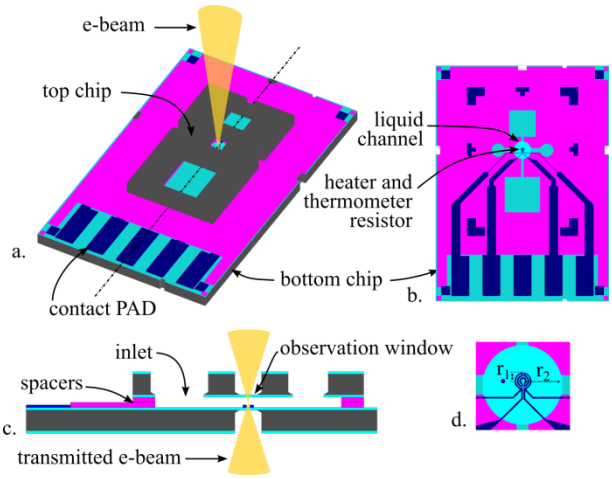

Figure 1: Schematics of the liquid cell, a. perspective view of the liquid cell, b. top view of the sole bottom chip, c. side view of the liquid cell with top and bottom chips stacked and aligned, d. zoomed view of the 4-wire resistive element. The liquid cell consists of two chips hermetically sealed. The top and bottom chips include free-standing thin (50-200 nm) silicon nitride membranes that aligned together form the observation chamber across which the electron beam of the TEM passes interacting with the studied specimen.

The devices are fabricated using clean-room micro-fabrication technologies as in [10].

Figure 2 (a) shows a top chip and a bottom stacked and aligned. The resistive element at the center of the observation chamber is visible through the transparent silicon nitride membranes. Before loading into the holder, the liquid cell is filled dropping the liquid sample over the inlet while the outlet allows gas to evacuate, then the liquid cell is hermetically sealed with UV-hardening epoxy and loaded into the sample holder as a static liquid cell. Figure 2 (b) shows an assembled liquid cell loaded into a sample holder with electrical contact. The holder is a custom designed holder with inserted wires enabling 5 electrical contacts. The presence of electrical contacts is the only requirement to be able to use this sealed liquid cell technology with integrated temperature control. The particular holder used here has no ability to flow liquid.

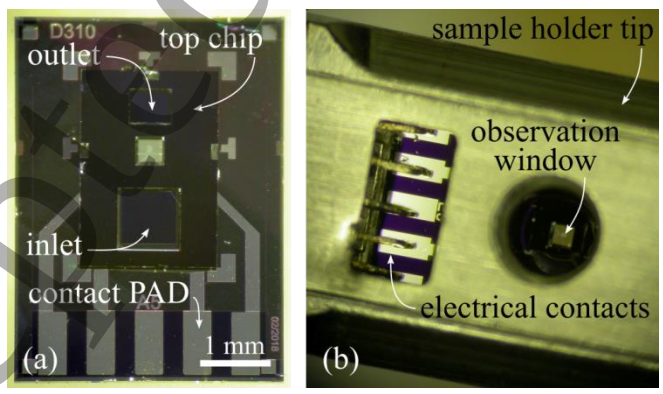

Figure 2: Pictures of realised devices. (a) Bottom and top chips stacked and aligned. (b) Liquid cell device loaded into a (S)TEM holder with electrical contacts.

2.2. Temperature control

The role of the temperature control is to enable the setting of a defined temperature at the location of the observation window independently of the device used and of the liquid filling the liquid cell.

A single resistive element is used for both temperature sensing through resistance variation measurement and heating with Joule power. The possibility to produce heat at the very same location of the temperature measurement with a single element, contrary to systems with separated heater and thermometer [18] favors a compact and simpler design and reduces the number of required pads.

The temperature control of this single resistive element is obtained with a heat feedback technique previously applied to infrared detectors [12] and gas sensors [14]; the capacitively coupled heat feedback technique. A detailed description of the digital version of the capacitively coupled electrical substitution technique can be found in [13]. The main principles and characteristics are summarized hereafter.

In this technique, the electrical bias point for temperature measurement and the Joule power signal for heating are separated in different frequency domains. The electrical bias point and consequently the temperature measure is at low frequency while the Joule power feedback signal is at high frequencies (several MegaHertz). This configuration allows independent configuration for the temperature measurement resolution and for the heating range. Figure 3 schematically illustrates the temperature control configuration. The resistive element is 4-wire. Two wires are used for the electrical biasing and coupled heat feedback and the other two wires are connected to an instrumentation amplifier for voltage measurement across the resistive element. The biasing resistor and the bias voltage at the output of a digital to analog converter are chosen to limit the elevation of temperature due to biasing power below 0.1°C. For example, in practice, V_{bias} is 1 V and R_{bias} 10 kOhm producing a maximum biasing Joule power of 1 µW in the resistive element. The instrumentation amplifier has a voltage gain of 1000 to take advantage of the full-scale voltage range of the component supplied by a symmetrical ±12 V power supply for a measurement range between room temperature and 100°C. The amplified and filtered signal is digitized for subsequent digital control processing with a Proportional Integral (PI) controller. A digital version, with a PWM (Pulsed Width Modulation) modulated output, of the capacitively coupled heat feedback technique is implemented to benefit from its intrinsic linearity that eases the PI controlled design [13]. The feedback PWM modulated signal is transposed at higher frequency with a carrier V_o at 3 MHz. The temperature setting for the desired working point is given to the controlled and the closed-loop system ensures that the desired temperature is reached. For the first practical implementation, a NI6251 acquisition board is used for the digital-to-analog, analog-to-digital and PWM functionalities. The PI controller is programmed in a Labview interface associated to the NI6215 acquisition board.

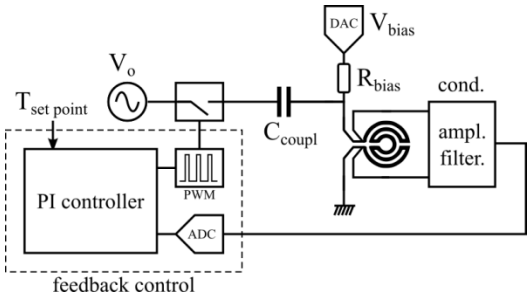

Figure 3: Temperature control scheme involving capacitively coupled electrical substitution.

Figure 4 shows an example of regular temperature cycling obtained with the temperature control implementation and a liquid cell. The set temperature cycle is a progressive ramp with 5°C steps of 30 s duration up to 85°C. Here, the response is damped to avoid overshoot and the response time to settle the temperature is set to 5 s with the conditioning electronics and PI controller. To visualize the temperature evolution the resistive element is covered with thermochromic ink (Thermochromic screen ink REF 47°C SFXC) [16]. The red color of this thermochromic ink turns transparent at temperature higher than 47°C. Picture insets for each temperature level are displayed next to the temperature axis. Two larger pictures illustrate the ink color state over the resistive element at 25°C and 85°C. From the temperature curve, a standard deviation of 0.11°C is calculated and noise analysis with a long time constant temperature setting yields to a $0.01°C^2/Hz$ white noise level in the working frequency range. The inset pictures with the red thermochromic ink allow visualizing the progressive temperature evolution around the resistive element and rather homogeneous behavior at the center of the membrane.

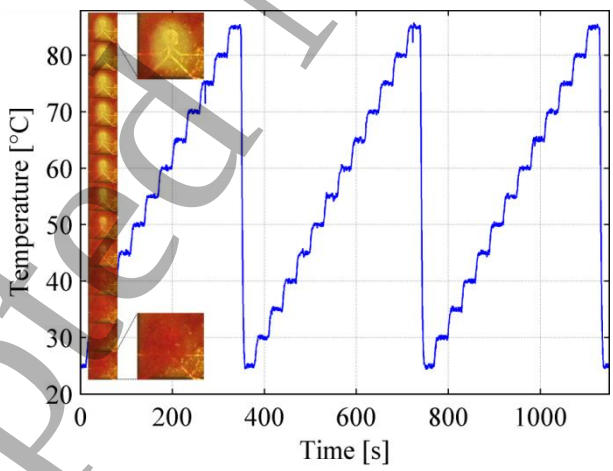

Figure 4: Temperature ramps with 5°C steps every 30 s up to 85°C. Inset pictures of the heater/temperature sensing resistive element covered with thermochromic ink for each temperature level are depicted next to the temperature axis.

Figure 5 illustrates an *in-situ* STEM heating experiment. PMMA (PolyMethyl MethAcrylate) polymer fragments are continuously observed while changing the temperature setting of the liquid cell. Figure 9(a) shows the fragments shape for temperature below 92°C. Figure 9(b) illustrates the fragments after

temperature setting over 92°C. The fragments have densified and present in rounded shapes. The temperature step lasts 15 minutes long but the shape evolution is observable right after the temperature increase (more precisely the shape evolution is observable after the re-focusing time of about 10 s required after the temperature increase). Considering the glass transition temperature of PMMA polymer ranges from 85°C to 165°C, the observed densification and rounding could be related to such a phase transition phenomenon. The pictures are taken in Z-contrast mode, also called dark-field mode. In this mode, the image is formed by scattered electrons collected by an annular detector and the contrast is directly related to the atomic number of the atoms being observed. Some small air bubbles, dark spots in the image, can appear during temperature experiments. Some are visible at the left-top side of Figure 9(b).

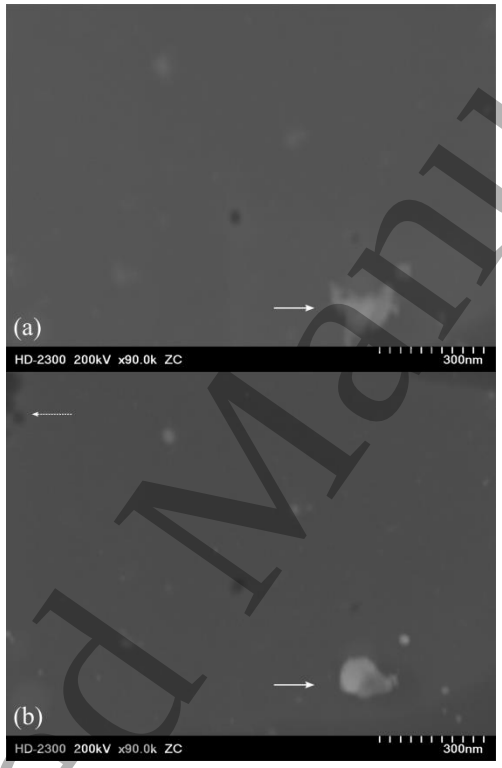

Figure 5: In Situ TEM thermal experiments, images in Z-contrast mode. (a) Polymer fragments for temperature below 92°C. (b) The same polymer fragments after 92°C has been exceeded. Magnification ×90k, scale bar 300 nm. The plain arrow in each figure indicates a polymer fragment. The dashed arrow points small bubbles that appeared during the heating.

4. Discussion

Equipping the liquid cell with temperature control capabilities will enable providing information at the nanoscale on real-time temperature effects on process dynamics. In life science, being able to study at the nanoscale biological specimen at 37°C is fundamental to have access to observation closer to real conditions. For material sciences, cycling temperature can provide a fast way to optimize liquid phase synthesis or to determine the effect of temperature on the growth or structuration of nanostructures

that ultimately impact their physical and chemical properties. The liquid cell with temperature control presented here answers such type of requirements with temperature control over the range room temperature up to 100°C. Future work will involve the usage of those temperature controlled liquid cells for *in-situ* TEM chemical experiments. Partial integration of the conditioning electronics and control will be investigated to miniaturize the experimental set-up and possibility to take advantage of faster temperature cycles, indeed such small liquid volumes in the observation window can be heated up with response time of the order of milliseconds or sub-milliseconds [17].

Temperature control adds to electrical biasing [10] and liquid actuation [18] previously developed to propose a set of on-chip functionalities for *in-situ* TEM studies.

3. Conclusion

In this paper, the design of liquid cell with temperature control is presented. Capacitively coupled heat feedback implementation ensures the temperature control of the liquid from room temperature to 100°C. The ability to control the temperature of a liquid sample while observing it in a TEM is a new capability that will enable providing information at the nanoscale on real-time temperature effects on process dynamics.

Acknowledgments

Some micro-fabrication process steps were done in the Takeda clean room at the University of Tokyo, partially financed by the MEXT Nanotechnology Platform.

References

[1] Marton L 1934 La microscopie électronique des objets biologiques, *Académie Royale de Belgique Bulletin de la Classe des Sciences*, **20**:439–46

[2] Abrams I M, McBain J W 1944 A closed cell for electron microscopy, *Journal of Applied Physics*, **15**:607–9

[3] He K, Bi X, Yaun Y, Foroozan T, Song B, Amine K, Lu J, Shahbazian-Yassar R 2018 Operando liquid cell electron microscopy of discharge and charge kinetics in lithium-oxygen batteries, *Nano Energy* **49**:338-345

[4] De Jonge N, Ross F M 2011 Electron Microscopy of specimens in liquid, *Nature Nanotech.* **6**:695-704

[5] Ross F 2015 Opportunities and challenges in liquid cell electron microscopy, *Sciences* **350**(6267), aaa9886

[6] Daulton T L, Little B J, Lowe K, Jones-Meehan J 2001 In Situ environmental cell-transmission electron microscopy study of microbial reduction of chromium (VI) using electron energy loss spectroscopy, *Microscopy and Microanalysis*, **7**, 470-485

[7] Krueger M, Berg S, Stone D A, Strelcov E, Dikin D A, Kim J, Cote, L J, Huang J, Kolmakov A 2001 Drop casted self assembling graphene oxide membranes for scanning electron microscopy on wet and dense gaseous samples, *ACS nano*, **5**(12), 10047-10054

[8] Grogan J M, Bau H H 2010 The Nanoaquarium: A Platform for *In Situ* Transmission Electron Microscopy in Liquid Media, *J. of Microelectromechanical Systems*, **19**(4), 885-894

[9] Zeng Z, Zhang X, Bustillo K, Niu K, Gammer C, Xu J, Zheng H 2015 In Situ Study of Lithiation and Delithiation of MoS2 Nanosheets Using Electrochemical Liquid Cell Transmission Electron Microscopy, *Nano Letters* **15**:5214-5220

[10] Egawa M, Ishida T, Jalabert L, Fujita H 2016, In-situ real time monitoring of nanoscale gold electroplating using micro-electromechanical systems liquid cell operating in transmission electron microscopy, *Applied Physics Letters*, **108**, 023104

[11] Creemer J F, Helveg S, Hoveling G H, Ullmann S, Molenbroek A M, Sarro P M, Zandbergen H W 2008, Atomic-scale electron microscopy at ambient pressure, *Ultramicroscopy*, **108**, 993-998

[12] Denoual M, Delaunay S, Robbes D, 2009 Bolometer with heat feedback, *WO/2009/034066*

[13] Denoual M, Lebargy S, Allègre G 2010 Digital implementation of the capacitively coupled electrical substitution for resistive bolometers *Meas. Sciences. Technol.* **21** 015205

[14] Denoual M, Robbes D, Inoue S, Mita Y, Grand J, Awala H, Mintova S 2017 Thermal resonant zeolite-based gas sensor, *Sensors and Actuators B: Chemical*, **245**, 179-182

[15] Carslaw H S and Jaeger J C 1959 Conduction of Heat in Solids (Oxford: Clarendon)

[16] Ueno R, Kim B J, Brioude A, Coleman A W 2015 Thermochromic ink as internal probes of thermal behavior in micro-fluidic systems, Proc. of MicroTAS Gyeongju, Korea, Oct 25-29

[17] Arata H F, Fujita H, 2009 Miniaturized thermocontrol devices enable analysis of biomolecular behavior on their timescales, second to millisecond, *Integrative Biology*, **1**, 363-370

[18] Denoual M, Menon V, Sato T, Fujita H 2017 On-chip fluidic actuation for TEM liquid cells, Proc. of Micro TAS, Savannah, Georgie, Oct 22-26